NOTES 6.

LIQUID CAVITATION IN FLUID FILM BEARINGS

Lecture 6 describes the phenomenon of liquid cavitation in steadily loaded fluid film bearings and notes the most adequate boundary conditions at the inception and reformation boundaries of the cavitation zone. The models developed to predict liquid cavitation model are detailed, from the simple Reynolds condition to the elaborate Jakobsson-Floberg-Olsson (*JFO*) model. Details follow on the *Universal Cavitation Algorithm* rendering a single Reynolds-like equation valid in both the full film (liquid) and cavitation zones. Issues of accuracy and stability when solving the single Reynolds equation for a variable known as the density ratio are highlighted. A digression related to dynamic liquid film cavitation applicable to squeeze film flows brings to attention the major differences with a steadily loaded (stationary) condition

Nomenclature

C	Bearing radial clearance. = R_B -R_J [m]
g	Switch function, =1 in full film zone, =0 in cavitation region
h	Film thickness [m]
h_*	Film thickness at inception (Start) of cavitation zone [m]
L	Bearing axial length [m].
M_x, M_z	Mass flow rates (per unit length) [kg/s/m]
M_*, M_η	$\rho_{cav}\, h_* \frac{\Omega R}{2}$. Mass flow rate into cavitation zone, flow at reformation boundary
P	Hydrodynamic pressure [N/m^2]
P_{amb}	Ambient pressure [N/m^2]
P_{cav}	Liquid cavitation pressure [N/m^2]
R	½ D. Bearing radius [m[
t	Time [s]
U	ΩR. Journal surface speed [m/s]
V	dh/dt. Squeeze film velocity [m/s]
$X= \theta R$, y, z	Coordinate system on plane of bearing
α	(ρ / ρ_{cav}). Density ratio
κ	$\rho \frac{\partial P}{\partial \rho}$. Liquid bulk-modulus [N/m^2]
ρ	Liquid density [kg/m^3]
ρ_{cav}	Density at P_{cav} [kg/m^3]
μ	Fluid absolute viscosity [N.s/m^2]
Ω	Journal angular speed (rad/s)
Subscripts	
*	Inception of the cavitation zone
a	Ambient value
cav	Cavitation

Introduction

Lubricants and process liquids making fluid film bearings reduce friction and wear, provide load capacity, and add damping to dissipate undesirable mechanical vibrations. Journal bearings and thrust bearings represent the vast majority of applications where the mechanical surfaces shear the fluid causing it to flow and to produce the *physical-wedge* where a hydrodynamic pressure generates to carry, without contact, an applied load (Hamrock, 1994).

Figure 6.1 shows a typical cylindrical journal bearing. Within the converging film region, the hydrodynamic pressure rises to a peak, decreasing to ambient pressure at the end sides and trailing edge of the thin film. In zones where the film thickness locally increases, the fluid pressure may drop to ambient, thus releasing the dissolved gases within the lubricant[1], or below ambient to its vapor pressure causing lubricant vaporization. The phenomenon of film rupture, characteristic of steadily loaded bearings, is known as *lubricant cavitation*, vaporous or gaseous, and its effects on the performance and stability of steadily loaded bearings are reasonably well understood and documented in the literature (Dowson et al., 1974, Brewe et al., 1990).

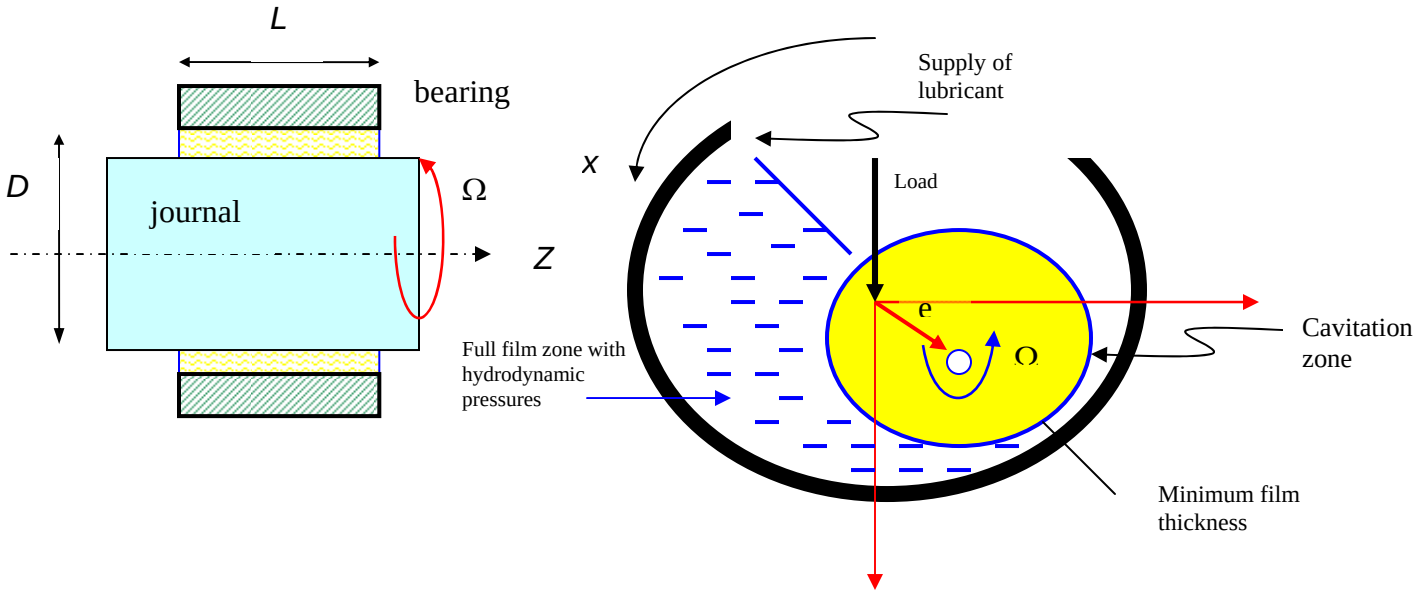

Figure 6.1. Cylindrical journal bearing showing lubricant cavitation

1 It is well known that liquids (under normal operating conditions) cannot sustain pressures below its saturation or vapor pressure (P_{sat}) since then the fluid vaporizes. On the other hand for pressures below ambient (~1 bar [14.7 psia]), the dissolved gases in a lubricant (air for example) are released. Streamers of flow coexist with vapor or gas generating the *cavitation region*. Most mineral oils contain between 8 and 12 % in volume of dissolved air (Pinkus, 1990).

Liquid cavitation in fluid film bearings is not only important because its onset and extent determine the load capacity of a fluid film bearing but also because vapor cavitation collapse (implosion) can cause severe surface material damage. Furthermore, in dynamically loaded bearings, the appearance of cavitation largely influences the rotordynamic stability of a rotor-bearing system and its maximum whirl amplitude of vibration (Brewe, 1986).

Dowson and Taylor (1974) provide a seminal discussion of the physical nature of liquid cavitation and the boundary condition models appropriate for thin film rupture. Brewe *et al.* (1990) also note the importance of bubble dynamics in bearing performance that affects the dynamic forced performance of an entire rotor-bearing system.

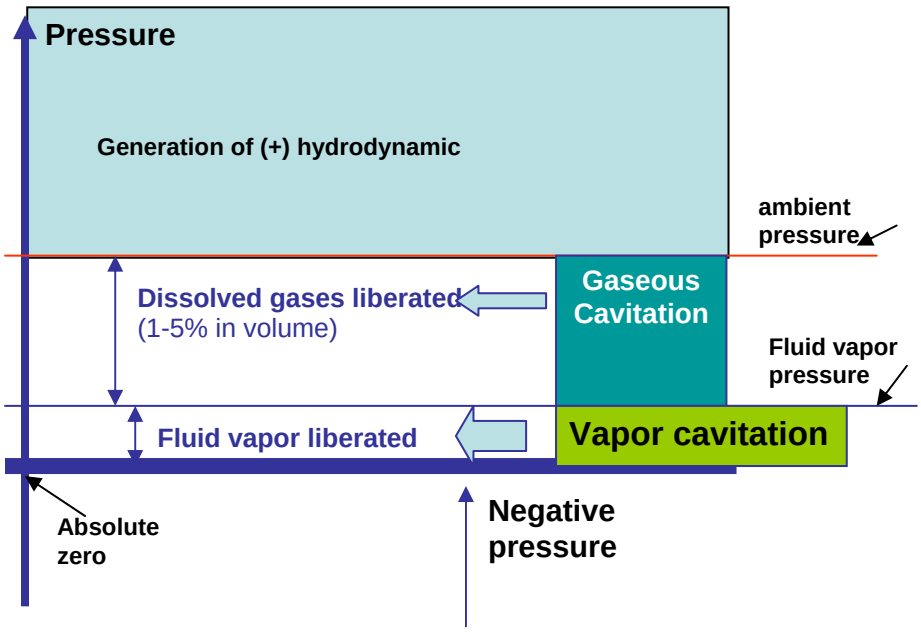

Diagram of liquid cavitation in fluid film bearings

Digression

Often fluid film bearings, and most notably squeeze film dampers (*SFDs*), carry large dynamic loads, transient or periodic, which cause the fluid in the film to go through local flow reversals. The fluid film pressure may fall repeatedly to ambient or even less to the lubricant vapor pressure if and only if the bearing is fully submerged in a lubricant bath.

However, in open end bearing configurations, the fluid does not only release its gaseous content, but it is more likely that the dynamic journal motion draws or ingests air into the lubricant film. Large amplitude journal motions at high frequencies then lead to the generation of *a bubbly mixture* (air in lubricant), which affects the bearing dynamic forced performance. The air entrapped as small bubbles clusters to make large striations. Bubbles may persist in the fluid film even in the zones of high dynamic pressure. Foamy oil at the damper outlet evidences this pervasive operating condition. Zeidan, et al. (1996) review the state of the art in *SFD*s and remark the importance of the air entrainment phenomenon, as it considerably reduces the dynamic squeeze film forces and the *SFD* overall damping capability. Diaz and San Andrés (1998, 1999) provide fundamental experimental measurements and an engineering model for prediction of the effects of air ingestion on the dynamic performance of squeeze film dampers. No accurate model has yet been forwarded for dynamically loaded journal bearings. See Notes 14 on squeeze film dampers for an extended discussion on

this topic.

Reynolds equation governs the generation of fluid pressure P within the full film region of thickness h. Under laminar and isothermal flow conditions and for an isoviscous liquid, Reynolds Eqn. is

$$\frac{\partial}{\partial t}\{\rho h\}+\frac{\partial}{\partial x}\left\{\frac{U}{2}\rho h\right\}=\frac{\partial}{\partial x}\left\{\frac{\rho h^3}{12\mu}\frac{\partial P}{\partial x}\right\}+\frac{\partial}{\partial z}\left\{\frac{\rho h^3}{12\mu}\frac{\partial P}{\partial z}\right\} \tag{6.1}$$

with $U=\Omega R$ as the surface speed of the rotating journal. Recall that the laminar mass flow rates per unit length are

$$M_x=-\frac{\rho h^3}{12\mu}\frac{\partial P}{\partial x}+\frac{\rho h U}{2};\quad M_z=-\frac{\rho h^3}{12\mu}\frac{\partial P}{\partial z} \tag{6.2}$$

Reynolds equation needs to be solved with appropriate boundary conditions at the cavitation zone.

The *Jakobsson- Floberg-Olsson* (*JFO*) film rupture (cavitation) model

Figure 6.2. View of gas cavitation region in a journal bearing

A film rupture model, based on mass flow continuity through the cavitation region, renders boundary conditions for the inception of the cavitation zone and the full film reformation boundary. Figure 6.2 shows a picture of a gas (air) cavity in a steadily loaded journal bearing. Note that within the cavitation zone the pressure, gas or vapor, is taken as constant.

At the inception of the cavitation zone, flow continuity requires a null pressure gradient with the pressure taking either ambient pressure or the fluid saturation vapor pressure. These conditions known as the ***Swift-Stieber* model** or simply as **Reynolds condition** do not warrant satisfaction of flow continuity in the cavitation zone except at its onset.

The ***flow separation* model** also considers lubricant motion in streamers, under or over the cavitation boundary, and derives a null velocity gradient to account for the inception of a secondary flow reversal. This flow detachment allows for the occurrence of subambient pressures as observed in some measurements.

The ***Floberg* model** postulates the conservation of liquid mass flow through the whole cavitation zone, but without mass transfer between the liquid lubricant and the vapor or gas bubble at uniform pressure (Floberg, 1961). In this model, a liquid of film thickness smaller than the local gap develops striations or streamers flowing parallel to the shear surface

velocity until a full liquid film develops again. The *Jakobsson-Floberg* model also accounts for fluid tensile strengths in the case of lightly loaded bearings (Dowson et al., 1974).

The ***Jakobsson- Floberg-Olsson (JFO) model*** applies to dynamic load situations in which the surfaces may also undergo (time varying) squeeze film motions (Floberg, 1974). The temporal change of the ruptured film volume is included in the liquid flow continuity equation and without consideration of the bubble dynamics. The boundary (shape) of the cavitation zone changes instantaneously as the surfaces squeeze speed changes, i.e. the phase change of liquid into vapor (or vice-versa) takes place at infinitesimally small times[2].

Figure 6.3 depicts possible configurations of the fluid flow through the cavitation zone as observed experimentally. Streamers attached to the runner surface (journal) carry the lubricant flow downstream of the cavitation inception point. In other observations, the whole journal surface appears wetted by a film of lubricant with the cavitation zone (bubble) attached to the stationary surface. The bottom sketch offers a depiction when both surfaces move and minute lubricant films adhere to both surfaces. Mistry et al. (1997) extended the *JFO* model to account for the balance of centrifugal force and surface tension in the weakly bonded streamers flowing with the journal surface.

2 Sun and Brewe (1992) note that the characteristic time for liquid vaporization (or vapor condensation) is very small when compared to the typical period of typical rotating machinery (> 1 ms), while on the other hand, the characteristic time for gas diffusion is orders of magnitude larger. Hence, the authors conclude that a dynamic cavitation bubble must contain fluid vapor since dissolved gases will not have enough time to come out of solution in a typical dynamic loading cycle. Braun and Hendricks (1984) measured the pressure and chemical contents within the cavitation zone in a steadily loaded, fully flooded journal bearing. These authors, however, noted the appearance of sub ambient pressures in the cavity zone formed by gasses coming out of solution from the lubricant. The authors argue that a phase change (oil vaporization) requires of a source of energy not readily available in actual operation.

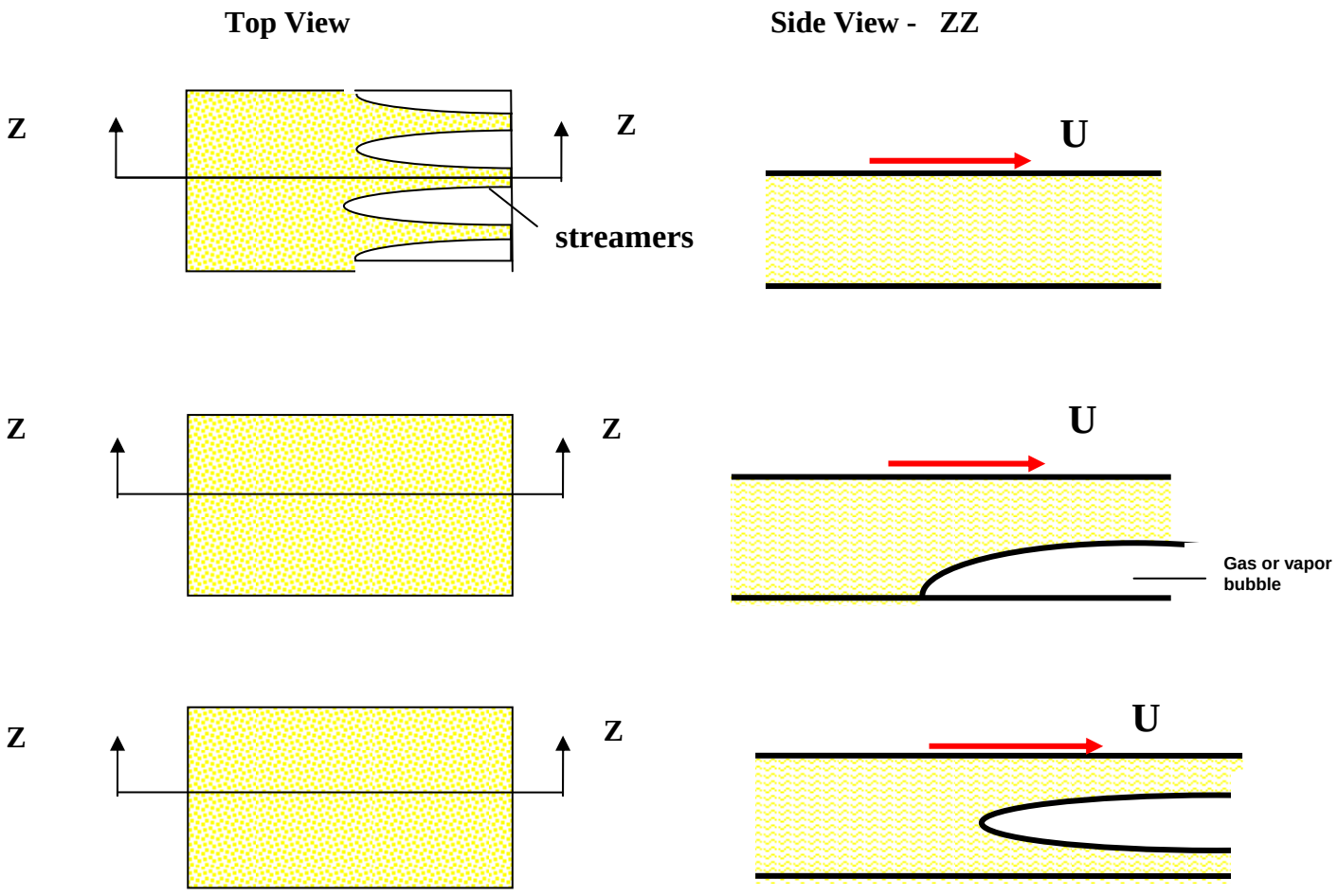

Figure 6.3. Fluid flow through cavitation zone

Figure 6.4 shows a schematic view of the inception boundary of the cavitation zone that is bounded by a film of lubricant moving with the journal surface. Within the cavitation region, the fluid pressure is uniform and equals a cavitation value, i.e.,

$$P(x, z, t) = P_{cav} \tag{6.3}$$

Thus, it follows that there is no pressure induced flow within this region, i.e., $\partial P/\partial x = \partial P/\partial z = 0$.

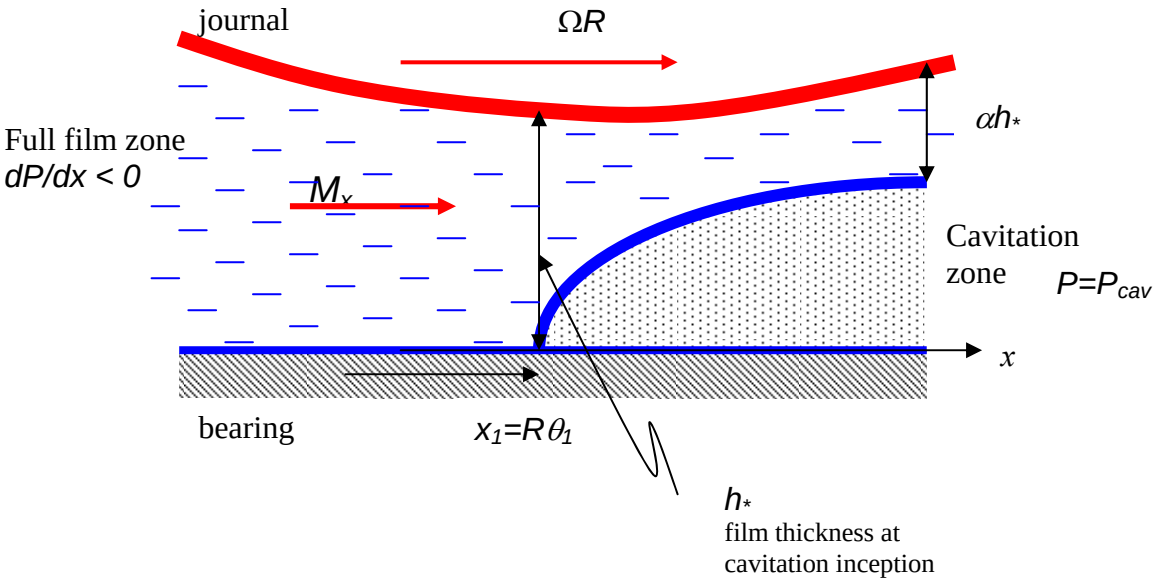

Figure 6.4. Cavitation inception in a thin film

The line $\theta_1(z_*)$ with film thickness h_* defines the leading edge (incipience angle) where the film ruptures. At the circumferential position, $\theta < \theta_1$, the pressure must be decreasing toward the cavitation value, i.e., $\partial P/\partial x < 0$. Hence, the local circumferential and axial flow rates are

$$M_{x_B} = -\frac{\rho\, h^3}{12\,\mu}\frac{\partial P}{R\,\partial\theta} + \rho\, h\frac{\Omega R}{2} \geq (\rho\, h)_*\frac{\Omega R}{2};\; M_{z_B} = -\frac{\rho\, h^3}{12\,\mu}\frac{\partial P}{\partial z} \tag{6.4}$$

and $h > h_*$. Within the cavitation region the liquid pressure is constant $(\partial P/\partial\theta = 0)$, and thus the liquid mass flow is

$$M_{xA} = \alpha\,\rho\, h\frac{\Omega R}{2} \leq \rho\, h_*\frac{\Omega R}{2},\; M_{zA} = 0; \text{and} \quad h > h_* \tag{6.5}$$

where α is known as a **fluid fraction content** at the cavitation zone, i.e. the ratio between the liquid volume to the total (liquid plus vapor) volume filling the film gap.

For steady loaded conditions (no temporal variations) the amount of liquid flow that enters into the cavitation zone must also leave, i.e. $flow_{in} = flow_{out}$. Hence, at the leading edge of the cavitation zone there can not be a flow discontinuity. Thus, it follows that the appropriate boundary condition (***Reynolds* condition or *Swift-Stieber* model**) at the leading edge of the cavitation zone are:

$$\left(\frac{\partial P}{\partial \theta}\right)_{\theta=\theta_1} = 0; \left(\frac{\partial P}{\partial z}\right)_{\theta=\theta_1} = 0 \tag{6.6}$$

Within the cavitation zone there is an amount of liquid flow transported in the circumferential direction,

$$M_* = \rho h_* \frac{\Omega R}{2} \tag{6.7}$$

where h_* is the film thickness at the inception of the cavitation zone (θ_l).

The model does not discern whether the transported flow is made of liquid streamers attached to the journal or whether the liquid fills part or the entire film gap. The distinction is not important unless the cavitation zone is a source or sink of thermal energy.

Film reformation occurs at the trailing edge of the cavitation zone (θ_t). At this boundary, a film of liquid fills completely the gap between the journal and the bearing; see Figure 6.5. Consider at the reformation boundary line Γ a small line element (Δs) with unit normal $\vec{\eta}$. From Figure 6.5, note that

$$\begin{aligned} &\vec{\eta} = \eta_x \vec{i} + \eta_z \vec{k}, \\ &\eta_x = \cos\alpha = \frac{\Delta z}{\Delta s}, \ \ \eta_z = \sin\alpha = -\frac{\Delta x}{\Delta s} \end{aligned} \tag{6.8}$$

Thus the flow entering the full film zone at the reformation boundary is

$$M_\eta = M_x \eta_x + M_z \eta_z = -\frac{\rho h^3}{12\mu}\frac{\partial P}{\partial \eta} + \rho \frac{\Omega R}{2}\eta_x \tag{6.9}$$

where $\dfrac{\partial P}{\partial \eta} = \dfrac{\partial P}{\partial x}\eta_x + \dfrac{\partial P}{\partial z}\eta_z$. And, to satisfy mass flow continuity, the flow leaving the cavitation zone must balance the flow entering the full film zone through the reformation line. That is

$$M_* \Delta z = \rho h_* \frac{\Omega R}{2}\Delta z = M_\eta \Delta s \tag{6.10}$$

and thus,

$$\left[-\left\{ \frac{\rho h^3}{12\mu}\frac{\partial P}{\partial x} + \frac{\rho h^3}{12\mu}\frac{\partial P}{\partial z}\left(\frac{-dx}{dz}\right)\right\} + \rho h \frac{\Omega R}{2} \right]_\Gamma = M_* \tag{6.11}$$

The solution of Eqn. (6.11) determines the slope (dx/dz) of the reformation line boundary (Γ), i.e. the coordinate (x) defining the cavitation boundary as a function of the axial position z. Note that to preserve flow continuity at the reformation boundary, there is a discontinuity in the pressure

gradient.

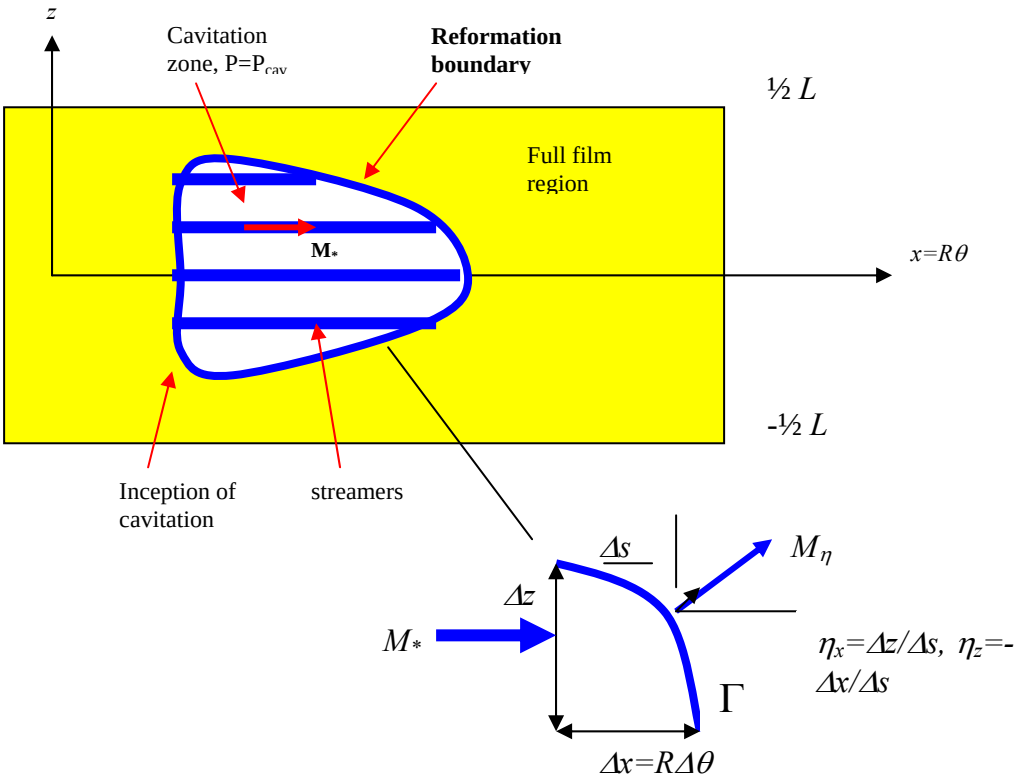

Figure 6.4. Flow balance at reformation boundary

Equations (6.6), (6.7) and (6.11), known as the ***JFO* model,** provide physically correct boundary conditions to solve the Reynolds equation in the full film zone. The *JFO* model applies to smooth surfaces and does not address to the material and thermo-mechanical aspects of liquid cavitation. For example, surface conditions play an important role in cavitation nuclei, i.e. crevices and surface roughness providing nuclei for vapor bubble inception and growth and leading to localized micro-spots of lubricant cavitation.

The ***JFO* model** predicts accurately[3] the onset and shape of the cavitation pattern in bearings operating with moderate to heavy loads (moderate to large journal eccentricities).

The ***JFO* model**, however, is not easily implemented in the (numerical) solution of Reynolds equation since the cavitation zone (inception and extent) is unknown a-priori. This condition is akin to the problem of determining a free surface in open flows, just as in liquid channel flows, sea waves, etc.

3 Etsion and Ludwig (1982) argue, in lieu of extensive experimental evidence in flooded journal bearings that the *JFO model* is not strictly in accordance with the observed physics within the film-rupture zone, namely the occurrence of subambient pressures and flow reversals.

Elrod and Adams (1974) and Elrod (1981) advance the ingenious ***universal cavitation algorithm*** where the *JFO* model is directly incorporated into a single Reynolds equation valid in both the full film zone and the cavitation zone. In the model, the lubricant pressure and density are related through the fluid bulk modulus (κ). A **switch function** (g=1 or 0) allows automatic satisfaction of the boundary conditions at the cavitation interface. The function also switches the character of the flow continuity (Reynolds) equation from elliptic to parabolic in the full film and cavitation regions, respectively. A variable (θ) is introduced for book keeping; $\theta \geq 1$, in the liquid (full film) region, and $\theta < 1$ in the rupture (cavitation) zone denotes a void or volume fraction (gas or vapor/liquid). The *universal cavitation algorithm* is detailed next.

Later developments have concentrated mainly on the implementation of fast and efficient numerical methods for the solution of the *Elrod algorithm* with applications to practical bearing configurations, and including dynamically loaded conditions. Brewe (1986), Woods and Brewe (1989), and Vijayaraghavan and Keith (1989) provide the most significant advances with continued refinements to the present day. However, the predicted pressure fields and cavitation extent depend greatly on the magnitude of the liquid bulk modulus (κ) used. In practice, artificially low values of the fluid bulk-modulus4, orders of magnitude lower than the typical value of 2.41 GPa for a mineral lubricant, are needed to "soften" the system of equations, to ensure numerical stability, and to avoid excessive round-off errors in the evaluation of the liquid pressure in the full film zone.

In general, the existing thin film rupture models are suitable to predict the onset, extent, and global shape of stationary enclosed vapor or gas cavities in steadily loaded, fully flooded bearings. The qualification of fully flooded or submerged operation is most important since in this case, ventilation to the (gaseous) ambient condition does not take place.

Consider, as depicted schematically in Figure 6.5, the flow evolution due to the sudden separation of two surfaces enclosing a thin film of lubricant. As the instantaneous film thickness increases with velocity $V=dh/dt > 0$, the fluid pressure drops and leads to the appearance of vapor (or gas) cavitation patterns (bubbles). Further motion of the top surface brings the formation of complex (dendritic) patterns as the bubbles expand and coalesce with others. Air (gas) from the surrounding may also be ingested into the film, eventually leading to the collapse of the thin film.

Before the ultimate rupture of the film, a sudden reversal in the top surface motion, $dh/dt < 0$, will expel some the bubbles out of the film as the instantaneous gap h begins to decrease. Further squeezing will generate hydrodynamic pressures and the ability to carry dynamic loads; the principle of squeeze film damping at work! For surface motions of periodic nature and at sufficiently high frequencies, the process leads to the ingestion and entrapment of gaseous media within the film, and the eventual formation of a bubbly non homogeneous mixture (Diaz and San Andrés, 1998, 1999). This important phenomenon is obviously not considered in the *JFO* cavitation model described.

4 The assumption may have a physical justification. Note that most liquids have an amount of dissolved gas content in them. Hence, the lubricant bulk modulus material property is lower than that of the pure fluid. See footnote (1): Most mineral oils contain between 8 and 12 % in volume of dissolved air (Pinkus, 1990).

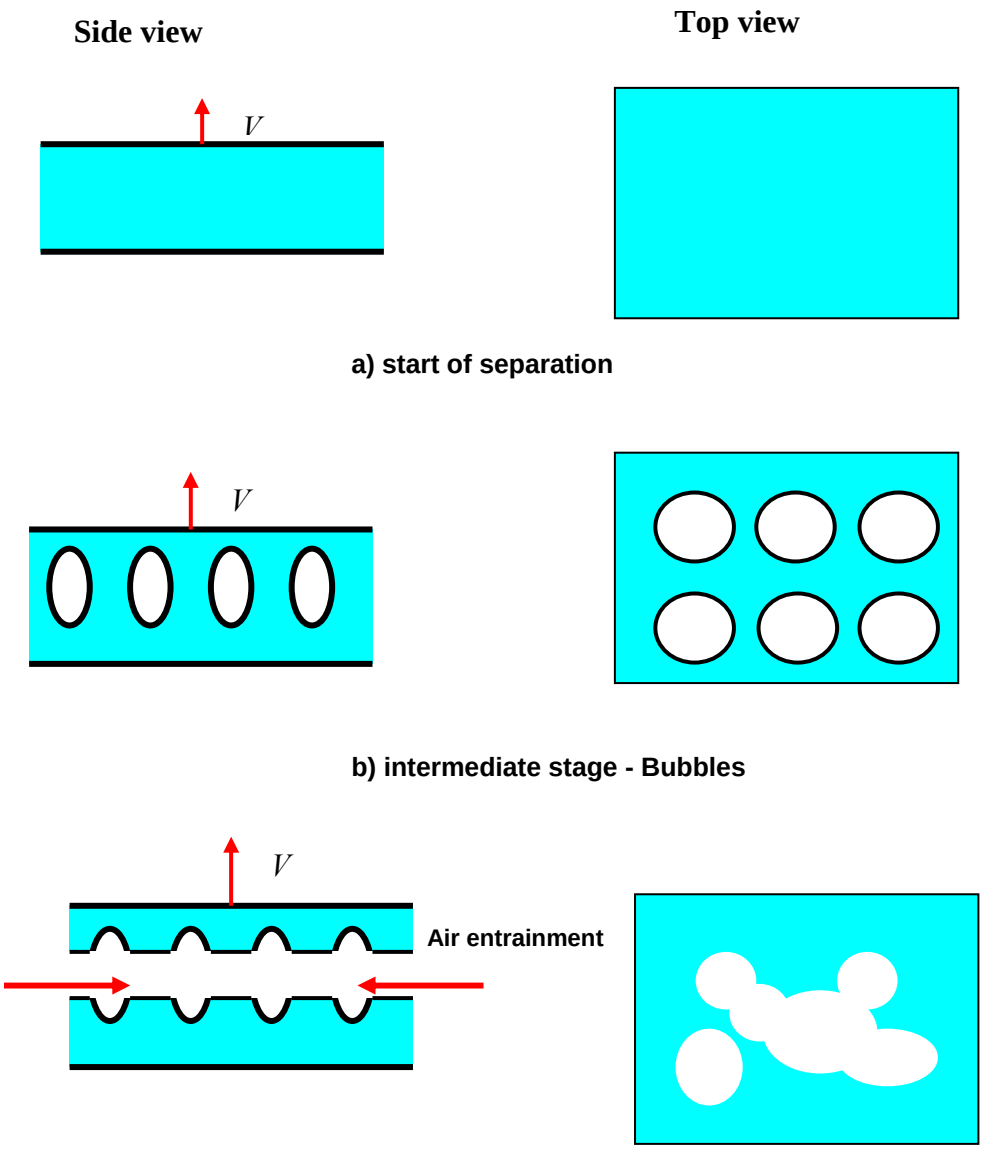

Figure 6.5. Progressive stages of dynamic liquid cavitation

A Universal Cavitation Algorithm:

The Elrod cavitation model avoids the tedious calculation of the cavitation boundary by reformulating the problem in terms of a new variable (different from pressure) and by developing a unique differential equation, applicable in both the full film region and the cavitation region. The algorithm also preserves mass conservation within the entire flow domain.

In a compressible liquid, the density is related to the pressure by the relationship:

$$\kappa = \rho \frac{\partial P}{\partial \rho} \tag{6.12}$$

where κ is the liquid bulk-modulus. Typical bulk modulus values for **pure** water and oil are ~2.01 and 2.41 GPa (292 and 350 kpsi), respectively.

Define $$\alpha = \frac{\rho}{\rho_{cav}} \tag{6.13}$$

As a density ratio, with ρ_{cav} is the liquid density at the cavitation pressure P_{cav}. Rewrite Eqn (6.13) as

$$g\,\kappa = \frac{\rho}{\rho_c}\frac{\partial P}{\partial(\rho/\rho_c)} = \alpha\,\frac{\partial P}{\partial \alpha} \tag{6.14}$$

where g is known as a **switch function**,

$$g = \begin{Bmatrix} 1 & \text{in full film zone} \\ 0 & \text{in cavitation zone} \end{Bmatrix} \tag{6.15}$$

Direct integration of equation (6.14) renders

$$P = P_{cav} + g\,\kappa\;\ell n(\alpha) \tag{6.16}$$

Note that in the full film region, g=1 and $P > P_{cav}$ since $\alpha = \frac{\rho}{\rho_c} > 1$; and in the cavitation region $P = P_{cav}$ since $g = 0$.

Incidentally, pressure differences (gradients) are of importance in thin film flows. Thus, for P_1 and P_2, both larger than P_{cav},

$$P_1 - P_2 = \kappa\left[\ell n(\alpha_1) - \ell n(\alpha_2)\right] \cong \kappa\left[\alpha_1 - \alpha_2\right] \tag{6.17}$$

Note that since (κ) has a large magnitude, small differences in density ratio *(α)* will cause large differences in pressure. This consideration may bring difficulties in the numerical model, hence the need to artificially reduce κ.

Vijayaraghavan and Keith (1989) point out that the variable α, although defined as the ratio of densities, has different interpretations in the full film and cavitation regions. In the former, $\alpha > 1$ since $\rho > \rho_c$ due to the compression of the lubricant. In the cavitation zone, $\alpha < 1$ for another reason. Within the cavitation zone, the lubricant density is uniformly (ρ_c) and the gap is not completely filled with lubricant due to the gaseous (or vapor) material within the cavity. Thus, α is termed the **fractional film content** and *(1-α)* represents the **void** (gas volume) **fraction.**

Recall that the conservation of mass flow in a thin film is

$$\frac{\partial(\rho h)}{\partial t} + \frac{\partial M_x}{\partial x} + \frac{\partial M_z}{\partial z} = 0 \tag{6.18}$$

where the components of liquid mass flow rate in the full film region are:

$$M_x = -\frac{\rho h^3}{12\mu}\frac{\partial P}{\partial x} + \frac{\rho h U}{2}; \quad M_z = -\frac{\rho h^3}{12\mu}\frac{\partial P}{\partial z} \tag{6.2}$$

while in the cavitation region, $\partial P/\partial x = \partial P/\partial z = 0$, and the mass flow rate within this zone is just

$$M_x = \alpha\,\rho_c\, h\frac{\Omega R}{2}; \quad M_z = 0 \tag{6.19}$$

Replacing $\partial P = \frac{\kappa}{\rho}\,\partial\rho = g\frac{\kappa}{\alpha}\partial\alpha$ into the mass flow rates, Eqn. (6.2), renders

$$M_x = -\frac{\rho_c h^3}{12\mu} g\kappa\frac{\partial\alpha}{\partial x} + \alpha\frac{\rho_c\, hU}{2}; \quad M_z = -\frac{\rho_c h^3}{12\mu} g\kappa\frac{\partial\alpha}{\partial z} \tag{6.20}$$

Note that these equations are valid in both flow regions since, in the full film zone $g = 1$ and $\alpha = \rho/\rho_{cav}$, and in the cavitation zone, $g = 0$ with α understood as the fractional liquid film content.

Substitution of the mass flow rates above into the global mass conservation Eqn. (6.18) gives

$$\frac{\partial}{\partial x}\left(\frac{\rho_c h^3}{12\mu} g\kappa\frac{\partial\alpha}{\partial x}\right) + \frac{\partial}{\partial z}\left(\frac{\rho_c h^3}{12\mu} g\kappa\frac{\partial\alpha}{\partial z}\right) = \rho_c\frac{\partial(\alpha h)}{\partial t} + \rho_c\frac{U}{2}\frac{\partial(\alpha h)}{\partial x} \tag{6.21}$$

This equation, where the α variable replaces the film pressure P, is valid everywhere within the flow domain. Note that in the *full film region*, $g = 1$ since $\alpha > 1$.

In the *cavitation region*, $\alpha < 1$, $g = 0$, and Eqn. (6.21) reduces to

$$\rho_c \frac{\partial(\alpha\, h)}{\partial t} + \rho_c \frac{U}{2} \frac{\partial(\alpha\, h)}{\partial x} = 0 \qquad (6.22)$$

thus establishing a dynamic flow balance in the cavitation zone.

Vijayaraghavan et al. (1989) discuss the numerical solution of Eqn. (6.21) to obtain the pressure field in cylindrical journal bearings. The model renders an elliptical finite (central) difference formula within the full film zone, and a hyperbolic formula (backward or upwinding difference) within the fluid cavitation zone.

Implementation of the *universal cavitation* algorithm in a computational program could lead to mixed success and little improvement over more crude techniques. The predictions will depend greatly on the magnitude of the bulk modulus(κ) used in the analysis. For example, realistic values of the lubricant bulk modulus (κ) render a system of algebraic equations **too stiff** for accurate solutions since small variations in density will produce very large changes in pressure in the full film zone. Thus, the numerical model is plagued with round-off errors.

To avoid the accuracy and slow convergence issues, analysts use an artificial low value of the bulk modulus, orders of magnitude smaller than the physical value. A numerically stable algorithm gives good results with κ values ranging from 1/100 to 1/10 of the actual physical magnitude. To conclude, computed results are problem dependent and the relevant literature is yet to report the details on a robust numerical procedure for the universal lubrication model.

Closure

The accompanying MATHCAD© program implements Elrod's algorithm for the solution of pressure in a one-dimensional slider bearing. The program displays results for calculations obtained using the simple Reynolds condition and the mass conservation model. The later model relies on point-wise under-relaxation since a line-solver produces numerical instabilities at the nodes where the cavitation zone starts and ends. Thus, the mass conservation model is both cumbersome and more computer intensive than the simpler model.

Extension of the computational model to two-dimensional bearing geometries is straight forward, although care must be taken with slow convergence at the cavitation inception boundary.

Use the program provided to assess the accuracy of the Reynolds condition model in relationship to the mass conservation model.

See Notes 14 for a lucid explanation on *dynamic* cavitation in journal bearings operating under large transient or periodic (dynamic) loads. The pervasive problems associated with air ingestion and entrapment in squeeze film dampers comes to light in the discussion.

References

Braun, M. J. and Hendricks, R. C., 1984, "An Experimental Investigation of the Vaporous/Gaseous Cavity Characteristics of an Eccentric Journal Bearing," *ASLE Lubrication Transactions*, Vol. 27, 1, pp. 1-14.

Brewe, D.E., 1986, "Theoretical Modeling of the Vapor Cavitation in Dynamically Loaded Journal Bearings," ASME *Journal of Tribology,* Vol. 108, pp. 628-638.

Brewe, D.E., Ball, J.H., and Khonsari, M.M., (editors), 1990, *Current Research in Cavitating Fluid Films, STLE Special Publication SP-28*.

Diaz, S., and San Andrés, L., 1998a, "Measurements of Pressure in a Squeeze Film Damper with an Air/Oil Bubbly Mixture," *STLE* Tribology Transactions, Vol. 41, 2, pp. 282-288.

Diaz, S., and San Andrés, L., 1998b, "Reduction of the Dynamic Load Capacity in a Squeeze Film Damper Operating with a Bubbly Lubricant," ASME Paper 98-GT-109.

Diaz, S., and San Andrés, L., 1999, "Air Entrainment and Lubricant Vaporization in SFDs: An Assessment of their Fundamental Differences," ASME Paper 99-GT-187.

Dowson, D., Godet, M., and Taylor, C.M., 1974, editors, *Cavitation and Related Phenomena in Lubrication,* ImechE, England.

Dowson, D., and Taylor, C.M., 1974, "Fundamental Aspects of Cavitation in Bearings," *Cavitation and Related Phenomena in Lubrication,* ImechE, England, pp. 15-26.

Elrod, H.G., 1981 "A Cavitation Algorithm," ASME *Journal of Lubrication Technology,* Vol. 103, pp. 350-354.

Elrod, H.G., and M. Adams, 1974, "A Computer Program for Cavitation and Starvation Problems," *Cavitation and Related Phenomena in Lubrication,* ImechE, England, pp. 37-42.

Etsion, I., and Ludwig, L.P., 1982, "Observation of Pressure Variation in the Cavitation Region of Submerged Journal Bearings," ASME *Journal of Lubrication Technology,* Vol. 104, pp. 157-167.

Floberg, L., 1961, "Experimental Investigation of Cavitation Regions in Journal Bearings," *Transactions of Chalmers University of Technology,* No. 238.

Floberg, L., 1974, "Cavitation Boundary Conditions with Regard to the Number of Streamers and Tensile Strength of the Liquid," *Cavitation and Related Phenomena in Lubrication,* ImechE, England, pp. 31-36.

Hamrock, B.J., 1994, *Fundamentals of Fluid Film Lubrication,* McGraw Hill Pubs, NY.

Mistry, K., Biswas, S., and Athre, K., 1997, "A New Theoretical Model for Analysis of the Fluid Film in the Cavitation Zone of a Journal Bearing," ASME *Journal of Tribology,* pp. 741-746.

Pinkus, O., 1990, "Thermal Aspects of Fluid Film Tribology," ASME Press, New York, pp. 317-326.

Sun, D. C., and Brewe, D. E., 1992, "Two Reference Time Scales for Studying the Dynamic Cavitation of Liquid Films," ASME *Journal of Tribology*, Vol. 114, pp. 612-615.

Vijayaraghavan, D., and Keith, T.G., 1989, "Development and Evaluation of a Cavitation Algorithm," *STLE Tribology Transactions,* Vol. 32, pp. 225-233.

Woods, C.M., and Brewe, D.E., 1989, "The Solution of the Elrod Algorithm for a Dynamically Loaded Journal Bearing Using Multigrid Techniques," ASME *Journal of Tribology,* Vol. 111, pp. 302-308.

Zeidan, F., San Andrés, L., and Vance, J.M., 1996, "Design and Application of Squeeze Film Dampers in Rotating Machinery," Proc. of the *25th Turbomachinery Symposium*, Texas A&M University, September, pp. 169-188.

One-dimensional Long Journal Bearing - Universal Cavitation Model (single point relaxation)

ORIGIN := 0

LSA 10/08/02 08/06 TAMU

The conservation of mass equation in the fluid film is:

$$\frac{d(m_X)}{dX} = \frac{d\left(\frac{-\rho}{\mu}\cdot\frac{H^3}{12}\cdot\frac{dP}{dX} + \rho\cdot H\cdot\frac{U}{2}\right)}{dX} = 0 \qquad \text{with} \quad h = \frac{H}{C} \quad x = \frac{X}{L} \quad p = \frac{P}{P_{ref}} \quad L = \pi\cdot D$$

In dimensionless form,

$$\frac{d(m_x)}{dx} = \frac{d\left(-\alpha\cdot h^3\cdot\frac{dp}{dx} + \alpha\cdot\Lambda\cdot h\right)\cdot\rho_c}{dx} = 0$$

with $h = 1 + \varepsilon\cdot\cos(\theta)$ and $\varepsilon = \frac{e}{C}$

is film thickness

journal eccentricity ratio

where: $\Lambda = \frac{6\cdot\mu\cdot U\cdot L}{C^2\cdot P_{ref}}$ is the bearing (speed) number

for a compressible liquid, the relation between density and pressure is: $K = \rho\cdot\frac{dP}{d\rho}$, where K is the bulk modulus. Then

$P = P_c + K\cdot\ln\left(\frac{\rho}{\rho_c}\right)$ with (Pc,ρc) as the pressure and density at set cavitation condition. define: $\alpha = \frac{\rho}{\rho_c}$

In dimensionless form: $p = p_c + \kappa\cdot g\cdot(\alpha - 1)$ since K is large. $\kappa = \frac{K}{P_{ref}}$

where g is a switch function, *g=1 in the full film zone, g=0 in the cavitation zone*

In the cavitation zone, α denotes the (void) volume fraction, i.e. the ratio between the lubricant film and the gap thickness.

Thus, the differential equation describing both the full film and cavitation zones is:

$$\frac{d\left(-g\cdot h^3\cdot\frac{d\alpha}{dx} + \alpha\cdot\Lambda_c\cdot h\right)}{dx} = 0$$

where $\Lambda_c = \frac{\Lambda}{\kappa}$ and boundary conditions p=p_{in}, p=p_{out} at x=0,1

SET BEARING PARAMETERS:

$\varepsilon := 0.270$ journal eccentricity

$\Lambda := 10$ (Bearing Number based on P_{ref}=14.7 psi)

$\kappa := \frac{100000}{14.7}$ dimensionless fluid Bulk modulus

$\Lambda_c := \frac{\Lambda}{\kappa}$ $\Lambda_c = 0.00147$

pressures at leading & trailing edge, cavitation pressure

$p_{in} := 0.0$ $p_{out} := p_{in}$ $p_c := 0.$

$error := 1.\cdot 10^{-8}$ (convergence error in film fraction)

$N := 99$ (Number of nodes in domain) of length L

$NITER := 600$ (Number of iterations in the solution of the non-linear equation)

Mesh & film thickness

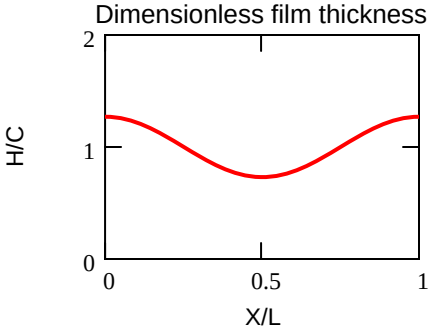

Solution procedures:

(a) **SolveNC**: finds guess pressure field from soln. of incompressible fluid Reynolds equation, with pressures below cavitation value neglected on back subsitution procedure, i.e. equivalent to setting the **Reynolds condition** (dp/dx)=0 at cavitation inception. Method: Direct soln. using TDMA.

(b) **Solve**: Finds solution of density fraction (α) using universal cavitation algorithm. Procedure performs a point-wise relaxation since TDMA does not work well and causes divergence.

Solution programs

(a) find pressure field with simple cavitation model (use as start field below)

$(p_{nc}\ \ \alpha) := SolveNC(p_{in}, p_{out})$

(b) solve using cavitation algorithm: FIX parameters

$(\alpha\ \ p\ \ g\ \ iter\ \ \alpha_{old}) := Solve(\alpha, p_{nc}, g, NITER, \beta)$

(c) Results:

iter = 600 iterations for convergence

$\max(\alpha) - 1 = 0.000082$

$\min(\alpha) = 0.669926$

$\max(p) = 0.556453$

$\min(p) = 0$

$\max(p_{nc}) = 0.46097$

$error = 1 \times 10^{-8}$

$p_c = 0$

(d) Graphical results

parameters: $\Lambda = 10$ $\varepsilon = 0.27$

$l := 0 .. N$

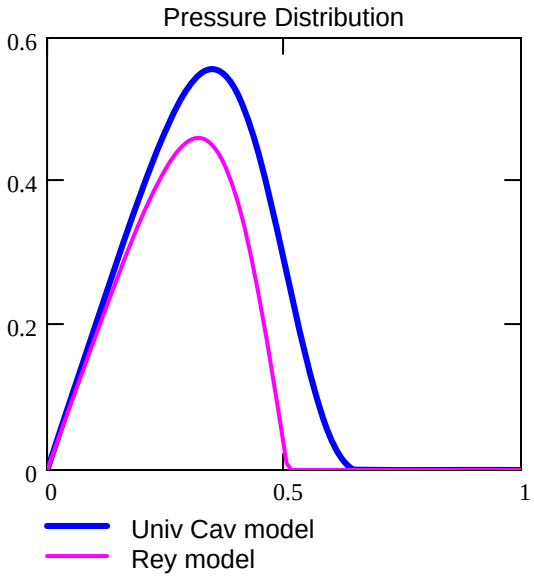

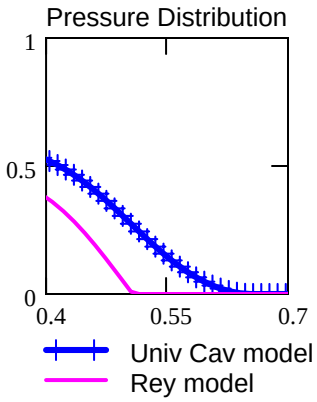

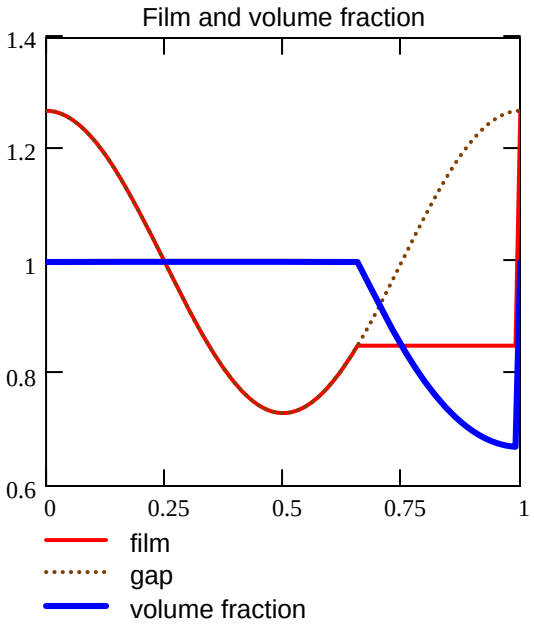

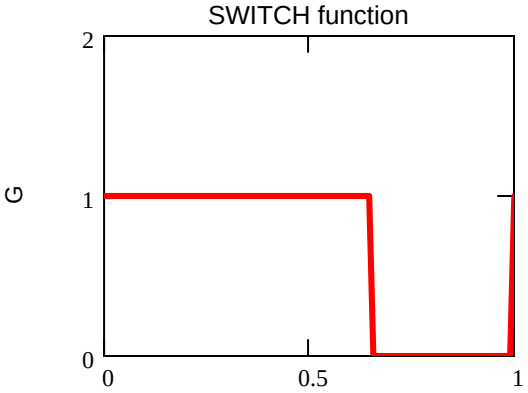

Note changes in peak pressure and shift of minimum pressure=pcav towards higher x (angles)

forces and flow rate

Forces from univ cav model and simple cavitation model

$\Lambda = 10$

$\varepsilon = 0.27$

$f = \begin{pmatrix} -0.061542 \\ 0.127757 \end{pmatrix}$ $f_{nc} = \begin{pmatrix} -0.022734 \\ 0.109949 \end{pmatrix}$ radial & tangential

$|f| = 0.141807$ $|f_{nc}| = 0.112274$ magnitude

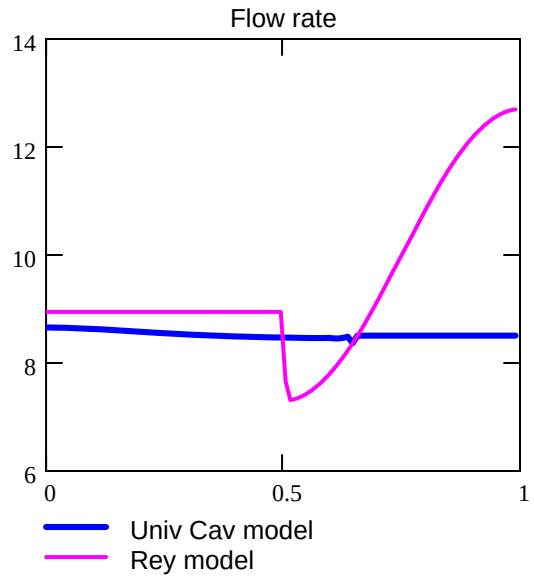

Compare mass flows from analysis
with sound cavitation model and one with out it!

Shear flow is excessive in cavitation zone since physical gap is equated to fluid film thickness.

The mass conservation model determines the corect volume fraction ratio.

$\max(M_x) = 8.656284$

$\min(M_x) = 8.364854$

Exercises:
Change parameters
oil : bulk modulus K, cavitation pressure Pc
operating conditions: speed Λ, end pressures, journal eccentricity ε

Find effect on pressure field, reaction forces and flow rate

Solution programs

(a) find pressure field with simple cavitation model (use as start field below)

$(p_{nc}\ \ \alpha) := \text{SolveNC}(p_{in}, p_{out})$

(b) solve using cavitation algorithm: FIX parameters

$(\alpha\ \ p\ \ g\ \ \text{iter}\ \ \alpha_{old}) := \text{Solve}(\alpha, p_{nc}, g, \text{NITER}, \beta)$

(c) Results:

iter = 600 iterations for convergence

$\max(\alpha) - 1 = 0.000349$

$\min(\alpha) = 0.222428$

$\max(p) = 2.373516$

$\min(p) = 0$

$\max(p_{nc}) = 2.034231$

$\text{error} = 1 \times 10^{-8}$

$p_c = 0$

(d) Graphical results

parameters:

$\Lambda = 10$

$\varepsilon = 0.7$

Large eccentricity

$l := 0 .. N$

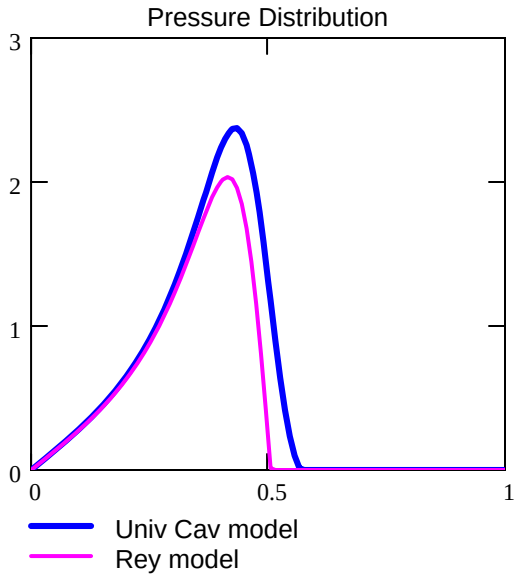

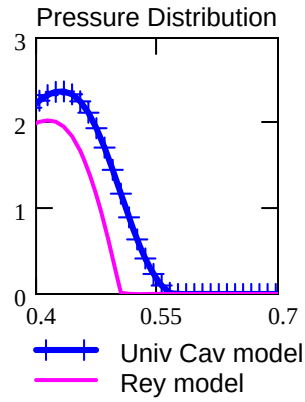

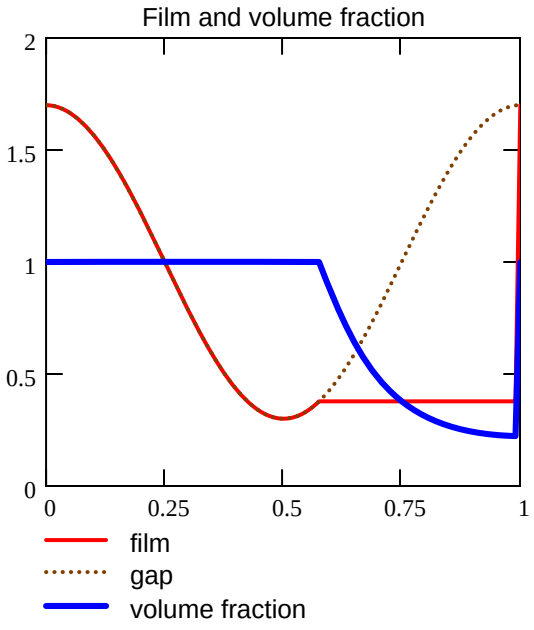

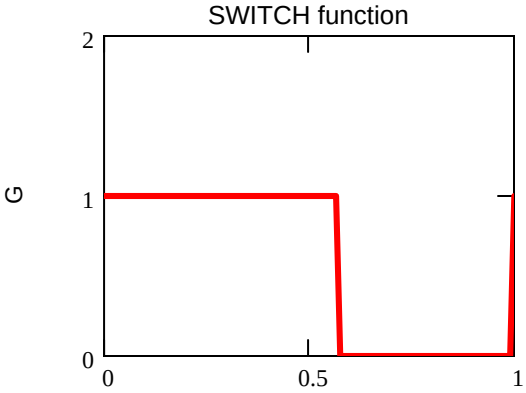

Note changes in peak pressure and shift of minimum pressure=pcav towards higher x (angles)

forces and flow rate

Forces from univ cav model and simple cavitation model

$\Lambda = 10$

$\varepsilon = 0.7$

$f = \begin{pmatrix} -0.302396 \\ 0.333442 \end{pmatrix}$ $f_{nc} = \begin{pmatrix} -0.205358 \\ 0.311175 \end{pmatrix}$ radial & tangential

$|f| = 0.450141$ $|f_{nc}| = 0.372829$ magnitude

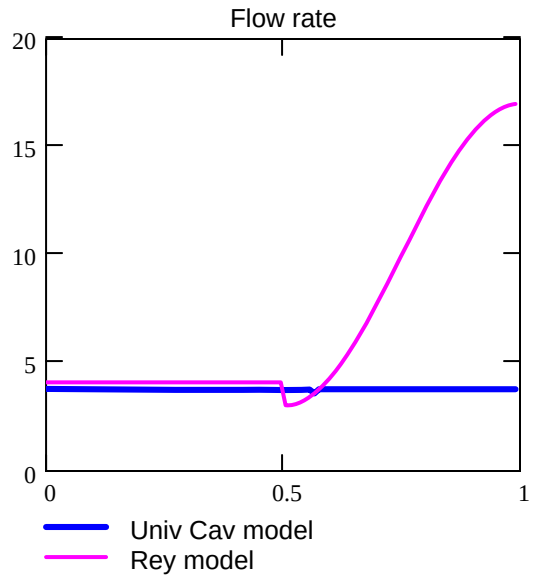

Compare mass flows from analysis
with sound cavitation model and one with out it!

Shear flow is excessive in cavitation zone since physical gap is equated to fluid film thickness.

The mass conservation model determines the corect volume fraction ratio.

$\max(M_x) = 3.793476$

$\min(M_x) = 3.587247$

Exercises:
Change parameters
oil : bulk modulus K, cavitation pressure Pc
operating conditions: speed Λ, end pressures, journal eccentricity ε

Find effect on pressure field, reaction forces and flow rate